Acta Cryst. (1982). A**38**, 408–413

Improvement of Electron Microscope Images by the Direct Phasing Method

BY K. ISHIZUKA, M. MIYAZAKI AND N. UYEDA

Institute for Chemical Research, Kyoto University, Uji, Kyoto-Fu 611, *Japan*

(*Received* 29 *July* 1981; *accepted* 11 *January* 1982)

Abstract

The resolution improvement and/or phase correction method devised for X-ray crystallography has been developed within the weak-scattering approximation for electron crystallography. Here the information of electron micrography and electron diffraction can be effectively combined. The usefulness of this method to improve the resolution and to improve the image quality has been demonstrated by test calculations. This method will be effective for radiation-sensitive materials, because it can work with only one micrograph and the diffraction data.

I. Introduction

The direct phase-determination method has been developed in X-ray crystallography (see Ladd & Palmer, 1980). In electron crystallography the dynamical scattering of electrons may prohibit the unlimited application of this method. However, Dorset & Hauptman (1976) have reported some successful results on the use of the direct phasing method based on phase invariants (Hauptman, 1972) for electron diffraction data. The applicability of the direct method to electron diffraction data has been investigated by Dorset, Jap, Ho & Glaeser (1979) using the Cowley–Moodie multislice formulation.

The phases of some reflections can be estimated from the electron micrograph, when a weak-scattering approximation is held (see Misell, 1978). This has been demonstrated by Unwin & Henderson (1975) for biological specimens and by Klug (1978/79) for an inorganic compound. An attempt to overcome the Scherzer limit has been implemented by Uyeda, Kirkland, Fujiyoshi & Siegel (1978) based on the method proposed by Schiske (1973) using several through-focus micrographs.

A resolution improvement and/or phase correction method was developed by Hoppe and his colleagues (Hoppe & Gassmann, 1968; Gassmann & Zechmeister, 1972; Gassmann, 1976) for X-ray crystallography. When this method is applied to electron crystallography, the information in the electron micrograph and electron diffraction can be effectively combined. In this research, we develop this method within the weak-scattering approximation and apply it to problems in electron crystallography. This method combined with the previously developed image reconstruction method (Uyeda & Ishizuka, 1975) will give a powerful tool for structure analysis of damage-sensitive specimens, since these methods work on only one micrograph together with an electron diffraction pattern.

II. Theoretical

The intensity distribution of the electron microscope image $I(\mathbf{r}_i)$ is given by the following equation:

$$I(\mathbf{r}_i) = 1 - i\varphi(\mathbf{r}_i) + i\varphi_i(\mathbf{r}_i), \qquad (1)$$

at the coordinate $\mathbf{r}_i$ in the image plane within the weak-scattering approximation. Here $\varphi_i(\mathbf{r}_i)$ is the amplitude of the scattered wave at the image plane.

The Fourier transform of this intensity can be described as follows (Uyeda & Ishizuka, 1975):

$$T(\mathbf{h}) = -2F(\mathbf{h}) \sin \chi(\mathbf{h})\, E(\mathbf{h})\, A(\mathbf{h}) \quad \text{for } \mathbf{h} \neq 0. \qquad (2)$$

Here $F(\mathbf{h})$ is the Fourier transform of the scattered wave at the bottom of the specimen of the coordinate $\mathbf{h}$ in reciprocal space. $A(\mathbf{h})$ is the aperture function and $\chi(\mathbf{h})$ is the aberration function of the form

$$\chi(\mathbf{h}) = \frac{2\pi}{\lambda}\left\{\frac{\Delta f}{2}(\lambda h)^2 - \frac{C_s}{4}(\lambda h)^4\right\}, \qquad (3)$$

where C_s is the spherical aberration coefficient, Δf is the defocusing value and λ is the wavelength of the incident electrons. $E(\mathbf{h})$ is a so-called envelope function (Wade & Frank, 1977) describing an attenuation of the contribution of each reflection on the image intensity from temporal and/or spatial coherency of electrons. The attenuation due to an energy spread of electrons (temporal partial coherence) is more important than that due to a finite electron-source size (spatial partial coherence) for a present-day high-resolution electron microscope equipped with a thermionic gun: The energy spread of accelerated electrons cannot be

0567-7394/82/040408-06$01.00

changed without replacing the electron gun, while the effective electron-source size can be changed by adjusting a condensor lens system. The envelope function due to the energy spread can be described as follows (Wade & Frank, 1977):

$$E(\mathbf{h}) = \exp -\{\pi\Delta(1/2)\,\lambda h^2\}^2, \qquad (4)$$

where Δ is a defocus spread converted from the energy spread ΔE: $\Delta f = C_c(\Delta E/E)$. C_c is a chromatic abberation coefficient and E is an acceleration voltage. Fig. 1 shows an example of $\sin\chi(\mathbf{h})E(\mathbf{h})$ for 500 kV electrons where C_s = 1 mm, Δf = 1000 Å and Δ = 150 Å. It should be noted that this function oscillates, goes to zero sometimes and is damped monotonically. $F(\mathbf{h})$ may be retrieved by dividing $T(\mathbf{h})$ by this function except the regions where $|\sin\chi(\mathbf{h})\,E(\mathbf{h})| \simeq 0$.

We have developed a method to phase the reflection in these regions, based on the procedure of phase correction summarized by Gassmann (1976). The outline of our method is shown in Fig. 2(*a*). Here the starting set $\mathbf{F}_o$ is constituted only by the structure factors whose amplitudes (F_o) and phases (α_o) are obtained from electron diffraction and the electron micrograph, respectively; that is, the starting set does not include the structure factors whose phases are not obtained from the electron micrographs, as mentioned before. The inverse Fourier transform of $\mathbf{F}_c$ ($\mathbf{F}_o$ at the first cycle) gives the potential distribution P_c which may differ from the real distribution, because some $\mathbf{F}_c$'s may not be included until this cycle or may be different from the real ones. This potential distribution P_c is modified according to a rule (the modification function in the direct space, MFD) to produce the more realistic potential distribution P_c^*. The Fourier transform of P_c^* will give $\mathbf{F}_c^*$ (amplitude F_c^* and phase α_c^*) a better structure factor than the previous $\mathbf{F}_c$. Finally, this structure factor $\mathbf{F}_c^*$ is modified according to another rule (the modification function in reciprocal space, MFR) which will give the improved new structure factor $\mathbf{F}_c$. In this step, some structure factors whose phases are reliably estimated will be included in the new set of $\mathbf{F}_c$ using the corresponding amplitude F_o obtained from electron diffraction. These procedures are repeated for ten to twenty cycles. In this cyclic procedure some new phases are automatically assigned and old phases are improved at the same time. It should be noted that both the modifications in the direct and reciprocal spaces are absolutely necessary. If either modification becomes inefficient at any cycle, the phase refinement is stopped after that cycle. The choice as well as the combination of the modification functions, MFD and MFR, is very important to get the improved phase information, or, in other words, the improved potential distribution.

The basic principle of modifying the potential distribution in direct space is to reduce peaks which are too high as well as to eliminate negative potential regions in order to represent the realistic potential distribution. Some modification functions examined in this report are shown in Fig. 2(*b*). A linear-form modification function MFD1 shown in Fig. 2(*b*) is used

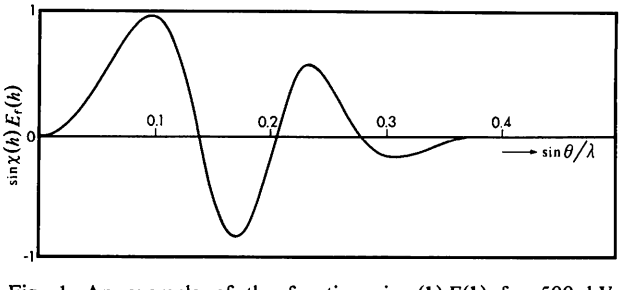

Fig. 1. An example of the function $\sin\chi(\mathbf{h})E(\mathbf{h})$ for 500 kV electrons where C_s = 1 mm, Δf = 1000 Å and Δ = 150 Å. Reliable phase information cannot be obtained from the electron micrographs when the absolute value of this function is small.

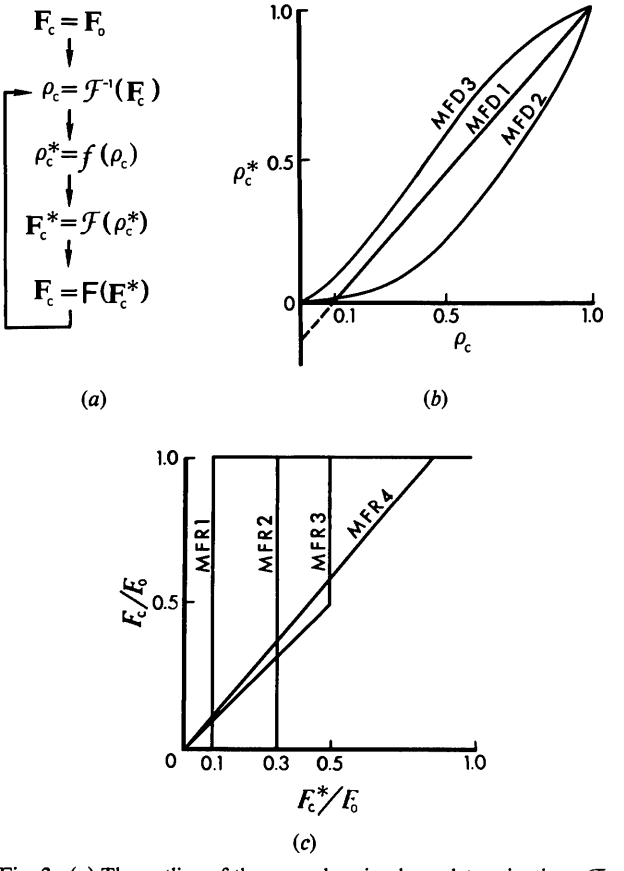

Fig. 2. (*a*) The outline of the procedure in phase determination. $\mathcal{F}$ and $\mathcal{F}^{-1}$ show the forward and backward Fourier transforms, respectively. f and F are the modification functions in real and reciprocal space, respectively. (*b*) The modification functions in direct space, MFD1 to MFD3 (see text). (*c*) The modification functions in reciprocal space, MFR1 to MFR4 (see text).

in this report. Gassmann & Zechmeister (1972) have found that a linear form leads to good results in the phase correction, even when the tangent formula does not correct the phases successfully. The tangent formula, which is used in reciprocal space, is closely related to the quadratic modification in direct space. However, the quadratic modification function MFD2 will be superior to the tangent formula, because the regions of negative potential can be suppressed to zero in direct space. The following cubic form has been proposed by Hoppe & Gassmann (1968) in the automatic phase expansion procedure in reciprocal space:

$$\rho_c^* = f(\rho_c) \equiv \frac{1-2T}{1-T}\rho_c + \frac{1+T}{1-T}\rho_c^2 + \frac{1}{1-T}\rho_c^3. \quad (5)$$

MFD3 in Fig. 2(*b*) is this type of function where $T = 0{\cdot}3$. ρ_c is normalized to unity in each cycle before applying these modification functions.

The modification in reciprocal space has been done by accepting newly calculated phases in the previously published papers as follows. According to Gassmann (1976), the newly calculated phase is accepted when $E_{cal}/E_{obs} \geq p$ and $E_{obs} \geq 1{\cdot}0$. Here E's are the amplitudes of normalized structure factors and p takes the value from 0·1 to 0·3. Karle (1968) has modified this p at each cycle taking into account the determined part of the structure. This modification function can be shown as MFR1 or MFR2 in Fig. 2(*c*), where $p = 0{\cdot}1$ and 0·3, respectively. These modifications are a sort of binary decision. In order to improve this nature, we have devised the linear modification functions which modified the amplitude as shown by MFR3 or MFR4 in Fig. 2(*c*). These are expressed as follows:

$$\text{MFR3: } \mathbf{F}_c = \begin{cases} F_o \exp(i\alpha_c^*) & \text{for } F_c^*/F_o \geq 0{\cdot}5 \\ F_c \exp(i\alpha_c^*) & \text{otherwise} \end{cases} \quad (6)$$

$$\text{MFR4: } \mathbf{F}_c^* = \text{MIN}(F_o, 1{\cdot}2F_c^*)\exp(i\alpha_c^*). \quad (7)$$

Other sophisticated higher-order modifications may work well, although we have not tried them in this investigation.

Since in electron crystallography the phase is determined from the Fourier transform of the electron micrograph, we use the normal structure factor F instead of the normalized structure factor E which is usually used in X-ray crystallography.

III. Results and discussions

Our procedure was applied to the model structure of the crystal of copper perchlorophthalocyanine $C_{32}N_8Cl_{16}Cu$ in a monoclinic form with the crystal data (Uyeda, Kobayashi, Suito, Harada & Watanabe, 1972): $a = 19{\cdot}62$, $b = 26{\cdot}04$, $c = 3{\cdot}76$ Å, $\beta = 116{\cdot}5°$.

A schematic representation of the structure projected along the c axis is shown in Fig. 3 where the plane symmetry is *cmm*. In this test calculation, we use the kinematical structure factors as F_o's, because the weak-scattering approximation is assumed. It has been shown on the basis of multislice calculations (Ishizuka & Uyeda, 1977) that large structure factors behave kinematically, up to certain thicknesses, although this molecule has many relatively heavy atoms.

A. Phase expansion

The phase expansion (the resolution improvement) was carried out from the resolution 1·67 to 1·0 Å (0·6 to 1·0 Å^{-1}). The amplitudes and phases (signs) of the structure factors within 0·6 Å^{-1} were used in the initial stage. The phases (signs) of the structure factors between 0·6 and 1·0 Å^{-1} were estimated assuming the amplitudes. In order to show which modification functions are suitable, two kinds of parameters were calculated: $R' = \sum |\mathbf{F}_o - \mathbf{F}_c| / \sum F_o$ and $R = \sum |F_o - F_c| / \sum F_o$. The parameter R' indicates the degree of the coincidence between the model (real) and calculated structures. However, this parameter cannot be calculated for the practical structure investigation, because the phases of $\mathbf{F}_o$'s are unknown. The parameter R can only be calculated for the unknown structure in the real application. If there is a good correlation between R and R', the convergence to the real structure can be estimated by the decrease in R. Hence good modification functions should give a small value of R', as well as a good correlation between R and R'. Fig. 4 shows the value of R' (*a* and *b*) and R (*c* and *d*) as a function of iteration cycle for each combination of MFD and MFR: MFD1 to 3 are shown by solid, dashed and dot-dashed lines, respectively, and MFR1 to 4 are indicated by a number on each line. Here the iteration has been stopped when the convergence takes place. In the case of MFR1 (Figs. 4*a*,*c*), the unreliable phases were also assigned and the correlation between R' and R was not good for all MFD's. On the other

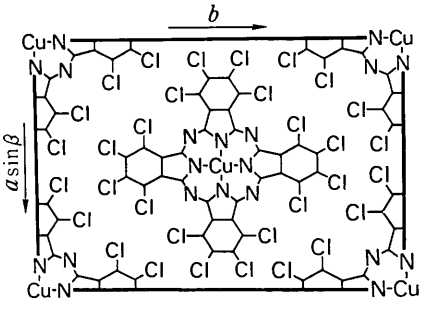

Fig. 3. A schematic representation of the model structure (copper perchlorophthalocyanine) projected along the c axis.

hand the phase assignment was difficult for MFR2 (*a* and *c*) except with MFD2. In the case of MFR3 (Figs. 4*b*,*d*), MFD1 and MFD3 gave good R' values. The correlation between R' and R was better for MFD1 than for MFD3. The same tendency as for MFR3 has been observed for MFR4 (*b* and *d*). In this case the amplitudes have been amplified 1·2 times in each cycle, so careful application will be necessary to avoid overphasing. It is concluded from the above results that the combination of MFD1 and MFR3 is the most suitable modification function. An example of the resolution improvement using these functions is shown in Fig. 5. At the eighth cycle (*d*), the image became similar to the 1·0 Å resolution image (*f*). Other phase expansions were carried out for resolutions 2·0 to 1·25 Å (0·5 to 0·8 Å^{-1}) and 2·5 to 1·67 Å (0·40 to 0·60 Å^{-1}). The best results were obtained with the combination of MFD1 and MFR3 (Fig. 6). The former case gives a relatively well improved result, while the

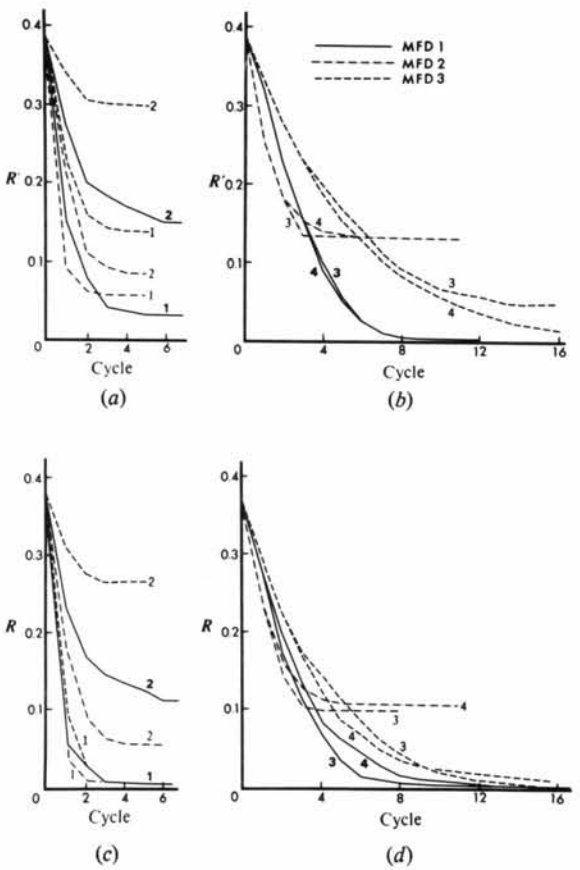

Fig. 4. The value of R' (*a* and *b*) and R (*c* and *d*) plotted as a function of iteration cycle for each combination of MFD and MFR. Solid, dashed and dot-dashed lines show MFD1 to 3, respectively. The number on each line indicates MFR1 to 4. The iteration was stopped when the value converged. The most suitable combination of the modification function should give the smallest value of R' as well as a good correlation between R and R'.

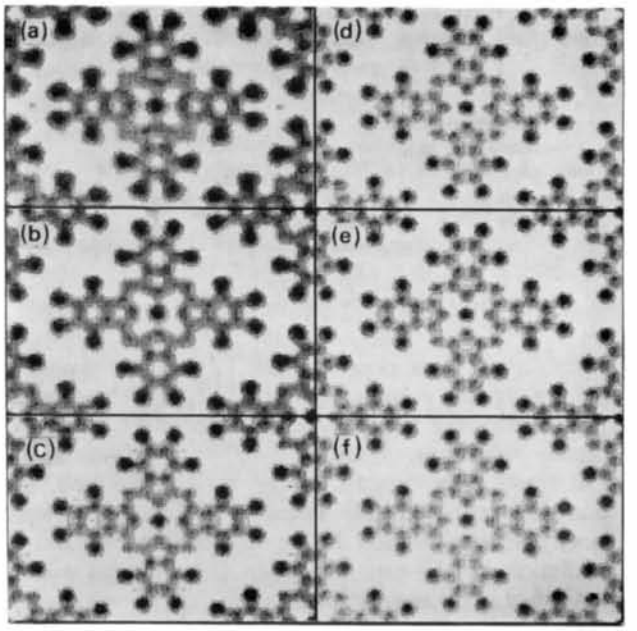

Fig. 5. An example of the resolution improvement from 1·67 to 1·0 Å (0·6 to 1·0 Å^{-1}). (*a*) An initial image of 1·67 Å resolution. (*b*) to (*e*) Some improved images at the second, fourth, eighth and 12th cycles, respectively. (*f*) The expected image of 1 Å resolution.

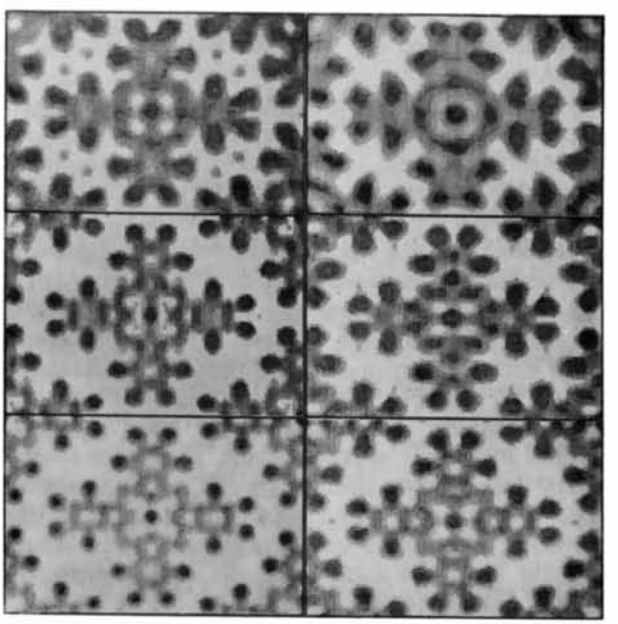

(*a*) (*b*)

Fig. 6. The results of the resolution improvement from (*a*) 2·0 to 1·25 Å and (*b*) 2·5 to 1·67 Å. In each case, top and bottom figures show the initial and expected resolution images, respectively. The image at the eighth cycle is shown at the middle.

Table 1. *Resolution improvement and related parameters for imaging characteristics of two different electron microscopes*

Case	Initial resolution h_i (Å^{-1})	Final resolution h_f (Å^{-1})	$\frac{h_f}{h_i}$	$R_i(R_i')$	R_f'	R_f	Q
I	0·6	1·0	1·7	0·39	0·00	0·00	0·24
II	0·5	0·8	1·6	0·43	0·09	0·05	0·38
III	0·4	0·6	1·5	0·43	0·22	0·04	0·51

improvement was poor for the latter case. Table 1 summarizes the parameters related to these three cases. The ratio of the intensity sum of the unknown to the known reflections, $\sum (F_o^{uk})^2/\sum (F_o^k)^2$, is shown as Q. The result may depend on the initial resolution, the extended ratio and the initial R. However, it may mostly depend on the ratio Q, and the improvement of resolution can be expected when $Q \leq 0{\cdot}4$ (as will be confirmed in the next section).

B. Phase interpolation

The phase interpolation is the procedure to determine the phases of the reflections for which $|\sin \chi(\mathbf{h})\, E(\mathbf{h})| \simeq 0$. The value of $\sin \chi E$ is dependent on the wavelength, the spherical aberration, the defocus and the defocus spread of the electron microscope. The following two conditions of the electron microscope are assumed: (*a*) 500 kV electrons: $C_s = 1$ mm, $\Delta = 140$ Å; (*b*) 200 kV electrons: $C_s = 1$ mm, $\Delta = 90$ Å. Here the resolution imposed by the defocus spread is 1·67 Å (0·6 Å^{-1}) for both cases, so these cases may be discussed on the same level of resolution. The phases (signs) of the reflections for which $|\sin \chi E| < 0{\cdot}2$ were regarded as unknown in this test calculation. The initial F_o which is assumed to be known takes the real phase (sign), *i.e.* the effect of a sign change of $\sin \chi$ has been corrected. The phase interpolation was carried out with the combination of the modification functions MFD1 and MFR3 which had given the most suitable results in the phase expansion. An example of the improvement of the image is shown in Fig. 7 for 500 kV electrons with a defocus of −1000 Å. It must be noted that the initial image (*a*) is remarkably improved from the original image with aberration (see Ishizuka & Uyeda, 1975), because the effect of $\sin \chi$ has been corrected from the outset. However, the improvement of the light-atom contrast is clearly observed in the image after the eighth or 12th cycle, (*d*) or (*e*), where the features similar to those of the theoretical image of 1·67 Å resolution (*f*) can be seen. The regions and the number of the unknown reflections change with the defocus value. The values of R' and R are plotted in Fig. 8 for the various defocuses. These parameters almost converged at about the tenth cycle. The values R' are plotted against the values R in Fig. 9(*a*). The correlation between R' and R is relatively good, which makes it possible to predict the improvement of images from the value of R. The image improvement depends on the defocus. This improvement might be expected when the initial R is less than 0·2 as can be seen from Fig. 8(*b*). However, some other cases, where the initial $R > 0{\cdot}2$, give also improved results. This can be more properly explained if we consider the ratio Q previously defined. The parameter R' is plotted against this ratio Q

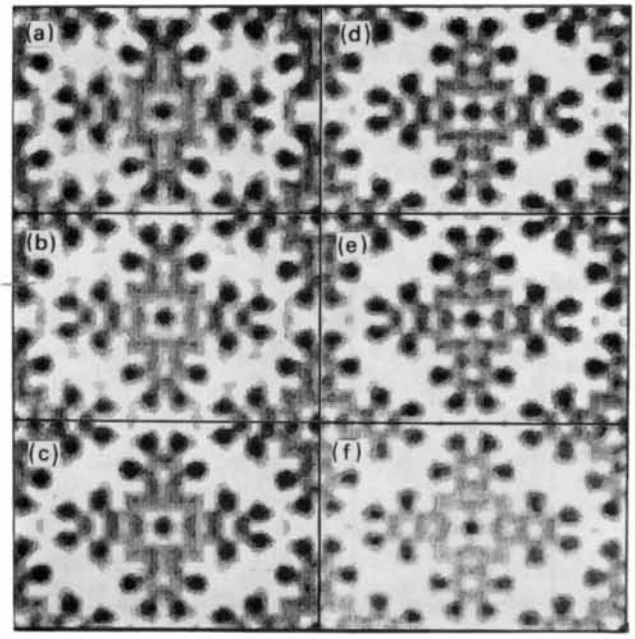

Fig. 7. An example of the image improvement for 500 kV electrons where $\Delta f = -1000$ Å, $C_s = 1$ mm and $\Delta = 150$ Å. (*a*) The initial image. (*b*) to (*e*) The improved image at the second, fourth, eighth and 12th cycles, respectively. (*f*) The image of 1·67 Å resolution.

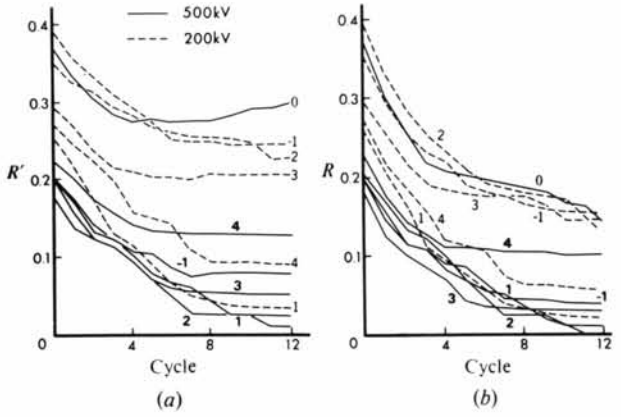

Fig. 8. The value of (*a*) R' and (*b*) R plotted as a function of iteration cycle for various defocuses. The defocus values are indicated in 10^3 Å unit. Solid and dashed lines show the results for 500 and 200 kV electrons, respectively.

in Fig. 9(*b*) for each defocus. It may be said that a good improvement will be expected when this ratio Q is less than about 0·4. It must be noted that the case of in-focus (0 defocus) data did not give good results, although it is near the best focus (Scherzer focus) where the good result is obtained. This can be explained that in the case of in-focus data there is a large region where $|\sin \chi E| \simeq 0$ at the center of the reciprocal space. Here the intensities of reflections are usually strong, and the ratio Q becomes large. The ratio Q for the case of 200 kV is usually larger than that for 500 kV, even though the resolution is the same (1·67 Å in our case). The superiority of 500 kV electrons over 200 kV electrons can be explained by this ratio Q.

IV. Conclusions

The usefulness of the phase assignment method in electron crystallography has been clearly demonstrated by the test calculation in this investigation. Here this method has been applied to the phase (sign) expansion (the resolution improvement) and the phase (sign) interpolation (the image improvement). A best combination of the modification functions is the linear form in both reciprocal and direct spaces. The apparent improvement has been observed when the ratio of the intensities of unknown to the known reflections is less than about 0·4. This method will be effective for radiation-sensitive materials such as biological specimens, because it can work on only one micrograph together with the diffraction data. The development of this method will be expected by the combination of the phase expansion and the phase interpolation.

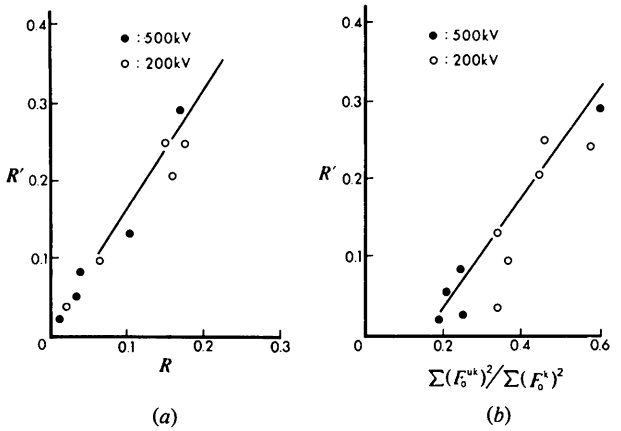

Fig. 9. (*a*) The correlation between the parameters R and R' (at the tenth cycle). (*b*) The correlation between $Q[\sum (F_o^{uk})^2/\sum (F_o^k)^2]$ and R' (at the tenth cycle). The correlation coefficients are 0·98 and 0·92 for (*a*) and (*b*), respectively.

The authors wish to thank Professor J. M. Cowley for his interest and for reading the manuscript. The work was supported by Grants-in-Aid (No. 843003) from the Ministry of Education, Science and Culture, Japan.

References

DORSET, D. L. & HAUPTMAN, H. A. (1976). *Ultramicroscopy*, **1**, 195–201.

DORSET, D. L., JAP, B. K., HO, M.-H. & GLAESER, R. M. (1979). *Acta Cryst.* A**35**, 1001–1009.

GASSMANN, J. (1976). In *Crystallographic Computing*, edited by F. R. AHMED, pp. 144–154. Copenhagen: Munksgaard.

GASSMANN, J. & ZECHMEISTER, K. (1972). *Acta Cryst.* A**28**, 270–280.

HAUPTMAN, H. A. (1972). *Crystal Structure Determination*. New York: Plenum Press.

HOPPE, W. & GASSMANN, J. (1968). *Acta Cryst.* B**24**, 97–107.

ISHIZUKA, K. & UYEDA, N. (1977). *Acta Cryst.* A**33**, 740–749.

KARLE, J. (1968). *Acta Cryst.* B**24**, 182–186.

KLUG, A. (1978/79). *Chem. Scr.* **14**, 245–256.

LADD, M. F. C. & PALMER, R. A. (1980). *Theory and Practice of the Direct Method in Crystallography*. New York: Plenum Press.

MISELL, D. L. (1978). *Adv. Opt. Electron Microsc.* **7**, 185–279.

SCHISKE, P. (1973). *Image Processing and Computer Aided Design in Electron Optics*, edited by P. W. HAWKES, pp. 82–90. London and New York: Academic Press.

UNWIN, P. N. T. & HENDERSON, R. (1975). *J. Mol. Biol.* **94**, 425–440.

UYEDA, N. & ISHIZUKA, K. (1975). *J. Electron Microsc.* **24**, 65–72.

UYEDA, N., KIRKLAND, E. T., FUJIYOSHI, Y. & SIEGEL, B. M. (1978). *Proceedings of the International Congress on Electron Microscopy*, Vol. 1, edited by J. M. STURGESS, pp. 220–221. Microscopical Society of Canada, Toronto.

UYEDA, N., KOBAYASHI, T., SUITO, E., HARADA, Y. & WATANABE, M. (1972). *J. Appl. Phys.* **43**, 5181–5189.

WADE, R. H. & FRANK, J. (1977). *Optik (Stuttgart)*, **49**, 81–92.